Fungal Ecology 79 (2026) 101472

Contents lists available at ScienceDirect

Fungal Ecology

journal homepage: www.elsevier.com/locate/funeco

Environmental regulation of *Hymenoscyphus fraxineus* apothecia development

Matt Combes [a,b,1,*], Lynne Boddy [b], Joan Webber [a]

[a] Forest Research, Farnham, Surrey, GU10 4LH, United Kingdom
[b] School of Biosciences, Cardiff University, Cardiff, CF103AX, United Kingdom

ARTICLE INFO

Handling Editor: Prof. Nicolai Vitt Meyling

Keywords:
Apothecia
Ascocarp
Ascomycete
Ash dieback
Environmental factors
Epidemiology
Fraxinus excelsior
Hymenoscyphus fraxineus
Invasive
Pathogen

ABSTRACT

Ash dieback, incited by *Hymenoscyphus fraxineus*, is causing mortality of ash across Europe. The pathogen colonises hosts via ascospores that are ejected from apothecia formed on ash leaf rachises, but information is lacking on the environmental factors that affect apothecia formation. This study, undertaken in England and Wales during summer 2018 and 2019, monitored the influence of temperature, relative humidity, ground cover, and canopy openness on apothecia development. Additionally, apothecia were monitored in the laboratory by incubating infected ash rachises at 4 °C, 10 °C, 15 °C and 20 °C, and then moving to 18–21 °C to assess how earlier incubation temperatures influenced subsequent apothecia formation. In the field, temperature had a positive effect on apothecia development which was amplified as relative humidity and canopy openness increased; ground cover associated with greater moisture also enhanced apothecia development. Laboratory investigations indicated a threshold temperature for apothecia formation of ~10 °C, with pre-incubation temperature influencing both the rate and probability of apothecia development.

1. Introduction

Symptoms of ash dieback disease were first noticed in Poland in the early 1990s with the causal agent identified almost a decade later (Kowalski, 2006), and since named as *Hymenoscyphus fraxineus* (Baral et al., 2014). An invasive ascomycete which originates from East Asia, the *H. fraxineus* population introduced into Europe shows divergence from the native population possibly due to hybridization with its European relative, *Hymenoscyphus albidus* (Buschbom, 2022). Ash dieback is currently affecting *Fraxinus* spp. (predominantly *F. excelsior* and *F. angustifolia*) throughout Europe, with survival across the continent broadly estimated at 50 % after three decades (George et al., 2022). Some individuals of European ash possess genetically based resistance, or tolerance, to the disease (McKinney et al., 2011; Enderle et al., 2014; Stocks et al., 2017), although environmental and stand variables such as temperature (Havrdová et al., 2017; Grosdidier et al., 2018), site moisture (Klesse et al., 2021), tree density (Grosdidier et al., 2020) and age (Havrdová et al., 2017; Grosdidier et al., 2020; Klesse et al., 2021) also affect disease outcomes.

The pathogen is aerially dispersed via ascospores that are ejected from apothecia and then cause infection when deposited on ash foliage or shoots. Germinating spores can enter the tree via enzymatic degradation of leaf epidermal cells, or penetrate lenticels on shoots or at the root collar (Husson et al., 2012; Cleary et al., 2013; Nemesio-Gorriz et al., 2019). If *H. fraxineus* colonises the leaf tissue, it forms a 'pseudosclerotial plate' on the infected ash leaf rachis (the compound leaf petiole) following leaf shed (Baral and Bemmann, 2014). This pseudosclerotial plate is highly resistant to biotic and abiotic degradation, thereby allowing *H. fraxineus* to persist within the litter layer and form apothecia on ash rachises usually in the following spring/summer when conditions are suitable (Queloz et al., 2011). Under laboratory conditions apothecia can develop for at least 5 years on rachises covered by pseudosclerotial plates (Kirisits, 2015).

Research into the ecology of the *H. fraxineus* life cycle has tended to focus on how environmental effects influence aerial spore release and ascospore density, rather than apothecia development. Currently, it is known that temperature (Chandelier et al., 2014; Čermáková et al., 2017; Hietala et al., 2018) and moisture indicators (Dvorak et al., 2015;

* Corresponding author. Warwick Crop Centre, School of Life Sciences, University of Warwick, Innovation Campus, Stratford-upon-Avon CV35 9 EF, United Kingdom.
E-mail address: matt.combes@warwick.ac.uk (M. Combes).
[1] Current address: Warwick Crop Centre, School of Life Sciences, University of Warwick, Innovation Campus, Stratford-upon-Avon CV35 9 EF, United Kingdom.

https://doi.org/10.1016/j.funeco.2025.101472
Received 30 April 2025; Received in revised form 31 August 2025; Accepted 11 September 2025
Available online 26 November 2025

Čermáková et al., 2017; Burns et al., 2022) are positively related to aerial ascospore density. Data on variables affecting the production of *H. fraxineus* apothecia are less precise, although most apothecia form during mid-summer (Mansfield et al., 2018), especially when sheltered under vegetation (Gross and Holdenrieder, 2013; Mansfield et al., 2018) and on sites with a higher flood risk index (Grosdidier et al., 2018). In contrast, their numbers can be limited by the availability of mating partners in sites with low infection, or where ash density is low (Laubray et al., 2023). More quantitative information on the environmental variables which influence apothecia development, including basic information such as temperature thresholds, is required to improve our understanding of ash dieback disease ecology.

More accurate estimates of the environmental regulators of the separate phases of the disease cycle would contribute to forecasting *H. fraxineus* infection risk through process-based models. This information can be used to guide surveys, as well as assess the impacts of disease control measures and effects of environmental change (Combes et al., 2024). In agricultural systems, such models have been developed with the aim of informing both disease assessments and application of treatments (Rossi et al., 2007; Caffi et al., 2011). Indeed, Bayesian inference has been used to produce a mechanistic model of the spread of *H. fraxineus* and ash dieback disease in France by utilising prior knowledge of the ash dieback disease cycle and associated parameter values (Fritsch et al., 2024). Inevitably however, the power of such models is influenced by the reliability of prior information and available data used for inference and validation.

The aim of this study therefore was to quantify effects of environment on *H. fraxineus* apothecia development through a combination of field and laboratory studies. Apothecia production and a range of environmental variables (temperature, canopy openness, ground cover, relative humidity) were monitored on up to seven sites in England and Wales throughout the spring/summer (May–September) across two consecutive years (2018 and 2019). Laboratory experiments were also used to examine the threshold temperature for *H. fraxineus* apothecia development and whether prior to this, a period of cool temperature exposure, such as might occur overwinter, was required to trigger apothecia formation. Separately, laboratory experiments explored the interaction between light and threshold temperatures for apothecia development. The findings of both field and laboratory approaches were then used to interpret how temperature, relative humidity, canopy openness and ground cover affect apothecia development in a woodland setting.

2. Materials and methods

2.1. Apothecia development in the field

2.1.1. Study locations

Seven *H. fraxineus* infected *F. excelsior* woodlands were selected based on two criteria. Firstly, the woodlands were geographically distanced to capture a gradient of long term temperature and precipitation from within England and Wales (Table 1; Fig. 1); secondly, they were accessible to volunteers who regularly collected sample material from each site. Apothecia were monitored at six of the sites during 2018, and all seven sites in 2019 (Table 1; Fig. 1). At each study site, four quadrats, which consisted of 13 grids (25 × 25 cm), were established at least 20 m apart. Quadrat locations were chosen to ensure that they were accessible for sample collection, minimise the risk of disturbance and to capture variations in ground cover. Twenty-five separate infected ash (*F. excelsior*) rachises were collected from the immediate vicinity of each quadrat (no more than 100 m^2 area with the quadrat as the focal point) and placed in each of the 13 grids of a quadrat. Rachises were identified on site as *H. fraxineus*-infected by the presence of a characteristic pseudosclerotial plate (Kowalski and Bilański, 2021), but the presence of the pathogen was subsequently verified for a subset of samples using the real-time PCR methods developed by Ioos et al. (2009a, 2009b) (File S1).

Table 1
Long-term (1979–2018) temperature and precipitation values at 1 km^2 resolution (Wouters, 2021) for experimental sites where *H. fraxineus* apothecia size was monitored from May–September 2018 and 2019.

Site	Grid ref.	Precipitation in warmest quarter (mm)	Mean temperature of warmest quarter (°C)	Years studied
County Durham (Hedley Hall Woods)	54.89736, −1.66161	214	14.61	2018, 2019
Shropshire (The Highfields)	52.84410, −2.46467	199	15.45	2018, 2019
Devon (Penstave Copse)	50.43512, −3.84455	197	15.23	2018, 2019
Wiltshire (Colerne Park and Monks Wood)	51.44945, −2.23595	197	15.83	2018, 2019
Hampshire (Alice Holt Forest)	51.15455, −0.85464	178	16.44	2018, 2019
Carmarthenshire (National Botanic Gardens of Wales)	51.83998, −4.15256	274	15.43	2018, 2019
Northumberland (Nunsbrough Wood)	54.93016, −2.07956	226	14.53	2019

2.1.2. Apothecia collection and measurements

At each site volunteers collected 25 *H. fraxineus* infected rachises from one randomly selected grid per quadrat at 1–2 wk intervals throughout the spring/summer (Table S1). The material was posted to the laboratory within 2 d of collection. Eight infected rachises were selected at random from each quadrat sample and apothecia removed from the lower 6 cm segment of each rachis (1 cm above the rachis base) and placed 'cup' down (Fig. S1) onto a thin layer of Vaseline on Petri dish bases in a fixed position for photography at either x1, x2, x3, x4, x5, or x6.3 magnification, depending on the size of the apothecia, using an Olympus SC100 Camera (Olympus, Tokyo, Japan) attached to a NIKON SMZ800 (Nikon, Tokyo, Japan) stereomicroscope. The mean diameter of apothecia was measured (two perpendicular measurements) to the nearest 10 μm either using microscope imaging software cellSens Dimension (Olympus, Version 1.7.1) or ImageJ software (Schneider et al., 2012). Apothecia were identified as *H. fraxineus* morphologically, but also verified molecularly in a subset of samples using real-time PCR methods developed by Ioos et al. (2009a, 2009b) (File S1).

2.1.3. Site characteristics

Data loggers (Tinytag Plus 2, Gemini Data Loggers UK) were positioned 40 cm above ground level in two locations at each site. The loggers recorded temperature and relative humidity every 10 min. Dominant ground cover of quadrats was classified as Vegetation, Litter, Moss or Soil. Areas with ground cover classified as vegetation were dominated by a range of herbaceous plants that shielded the litter layer below. In the litter classification, the litter layer was exposed and usually consisted of mixed broadleaf litter except at Carmarthenshire D, where it included bamboo (Bambusoideae) litter, whilst other ground cover types either consisted of moss or bare soil with limited leaf litter or plant growth. Hemispherical photographs of the overhead tree canopy were taken at 1.3 m above each quadrat using a Canon EOS 50D camera with Sigma 4.5 mm f/2.8 EX DC HSM fisheye lens attached and mounted on SLM9 self-levelling mount (Delta-T Devices, Cambridge). The photographs were taken during July and August 2020 at all locations except Hampshire location A and D (Table S2) which was photographed in 2018 prior to felling in 2019. The gap fraction, a measure of canopy openness based on the proportion of unobstructed visible sky (cf. Gonsamo et al., 2013), was then calculated using HemiView software version 2.1 (Delta-T devices, 1999).

Fig. 1. Locations of field experimental sites. 1 = Devon; 2 = Hampshire; 3 = Wiltshire; 4 = Carmarthenshire; 5 = Shropshire; 6 = County Durham; 7 = Northumberland.

2.1.4. Statistical analyses

Only apothecia > 200 μm diameter were used in the analyses, as smaller apothecia could not be sampled reliably and also did not have a visible spore bearing surface (hymenium) (Fig. S1). The total apothecia area (approximated using πr^2) from a quadrat on a given sampling date was then calculated for use in further analyses. The data were analysed using R software version 4.1.1 stats (R Core Team, 2021), lme4 (Bates et al., 2015), lmerTest (Kuznetsova et al., 2017), MuMIn (Barton, 2020), qpcR (Spiess, 2018), car (Fox and Weisberg, 2019), emmeans (Length, 2021), merTools (Knowles and Frederick, 2020), DHARMa (Hartig, 2021), ggplot2 (Wickham, 2016) packages. Nested linear mixed effects models were fitted with site, quadrat and sampling year all defined as random effects, and with quadrats nested within sites. This allowed the examination of both site and quadrat level variables, whilst controlling for unaccounted variance between sites, quadrats and sampling years. The square root of the total apothecia area was taken to meet the linear response assumption of the model. The $\log_{10}$ of the square root of the total apothecia area (μm^2) was ultimately used as the response variable in models and zero values were removed to meet model assumptions of a normal distribution of residuals.

Maximal nested linear mixed effects models were constructed for mean temperature interacting with mean relative humidity and ground cover. Models were also constructed replacing ground cover with gap fraction. These variables were modelled separately due to high covariance. Mean relative humidity and temperature were measured from 7 to 42 d prior to collection at 7 d intervals. Fewer sampling weeks were assessed at some sites because of late set-up of data loggers (Table S1). All continuous explanatory variables were brought onto a comparable scale for model construction by subtracting the mean and dividing the standard deviation from a given value.

The maximal nested linear mixed effects models, fitted using REML (restricted/residual maximum likelihood), were subject to stepwise reduction of non-significant effects using Kenward-Roger approximation for denominator degrees of freedom (Luke, 2017), and 0.01 as a threshold value for significance. The reduced models containing significant variables were fitted with ML (maximum likelihood), and AICc (second-order Akaike Information Criterion) values then calculated to provide a relative measure of model performance based on Kullback-Leibler information (Hurvich and Tsai, 1989). Models were compared using ΔAICc values, which quantifies information loss of models relative to the most supported model. Models with ΔAICc values of less than 7 were considered plausible (Burnham et al., 2011).

Data could not be analysed with site as a random effect for models that included gap fraction, due to the insufficient spread of gap fraction values between sites. However, the site was included in these models as a fixed effect to account for between site variation. Likelihood ratio tests of models (fitted using ML) and ΔAICc (i.e. less than 7) were then used to examine the effect of removing site as a random effect from models where fitting this random effect was possible (i.e. models including ground cover). When site could be removed as a random effect without significantly affecting these models, then the performance of fixed effects in gap fraction models and ground cover models could be compared (via ΔAICc values) with site fitted as a fixed effect.

Most supported models (ΔAICc values less than 7) were then fitted using REML to describe model features. The interactions in models were examined by calculating the estimated marginal mean of the $\log_{10}(\sqrt{}$(-total apothecia area)) within measured ranges of the explanatory variables, using Kenward-Roger approximation for denominator degrees of freedom (ddf). The variance explained by fixed effects in these models was represented using marginal R^2 values, and the variance explained by both fixed effects and random effects was represented using conditional R^2 values (Nakagawa and Schielzeth, 2013).

2.2. Apothecia development in the laboratory

2.2.1. Effect of incubation temperature

Fraxinus excelsior rachises with *H. fraxineus* pseudosclerotial plates were collected from Queen Elizabeth Country Park, Hampshire in March 2018, placed in sealed plastic bags, and stored at 4 °C for 3 d prior to the start of experiments.

A 4 cm segment was cut 1 cm above the base of each individual rachis, and then batches of rachises were submerged in water for 2 s and placed in sealed plastic boxes (17 cm length x 10 cm width x 4.5 cm height) lined with wet paper towels to maintain high humidity. Boxes each contained 13 to 16, 4 cm long rachis segments, and were incubated in darkness at 4, 10, 15 or 20 °C (7 replicate boxes per temperature). After 5 wks, visual assessment of each rachis segment was conducted at 1–2 wk intervals over a further 12 wks, by which time apothecia were

starting to senesce. The number of rachis segments on which immature apothecia (consisting of only a stipe; Fig. S1) and mature apothecia (stipe and spore bearing cup; Fig. S1) developed was recorded for each box. Only white immature and mature apothecia were recorded, as darker coloured structures were considered senescing and non-viable.

2.2.2. Effect of previous incubation temperature

After 17 wks incubation in darkness at the range of temperatures described in 2.2.1, boxes were removed from incubators, opened briefly to reoxygenate, and moved into the laboratory (18–21 °C) where they were exposed to daylight (but out of direct sunlight) by placing the transparent sealed plastic boxes approximately 5 m away from a west south west facing large (~2 m x ~1.5 m) glass window at a perpendicular angle beginning on July 20, 2019. LED lighting on the laboratory ceiling (~2 m from boxes) also typically augmented the daylight for ~8 h per day 5 days per week. The formation of new apothecia was monitored at 1–2 wk intervals starting 3 wks after removal from incubators and concluded after 19 wks. Sampled rachis numbers differed to those described in 2.2.1 as some rachis segments were removed for real-time PCR testing and others for photography. In total, 6 boxes remained for rachis assessment that had previously been incubated at 4 °C, 10 °C and 20 °C, and 5 boxes that had previously been incubated at 15 °C. The number of rachises within each box ranged from 9 to 14.

2.2.3. Interaction between light and threshold temperature

Hymenoscyphus fraxineus infected rachises were collected from Alice Holt Forest (Table 1) in February 2021 and stored at 4 °C for 6 months until experimentation. Seven replicate boxes, each containing 15 rachises, were then incubated at 10 °C under a 16h/8h (day/night) cycle (20,000 lx; MLR-351, Sanyo, Japan), or at 10 °C wrapped in foil to keep in darkness. The total number of boxes in each treatment was reduced (4 boxes at 10 °C in light; 6 boxes at 10 °C in dark) due to improper sealing of boxes which led to drying during the experiment. Temperatures inside the boxes were validated using data loggers (Tinytag Plus 2, Gemini Data Loggers UK) over a 72 h period. Numbers of developing apothecia were recorded after 9 wks of incubation under day/night conditions, and after 19 wks of incubation in constant darkness.

2.2.4. Statistical analyses

The data were also analysed using R software version 4.1.1 stats (R Core Team, 2021) and packages DHARMa (Hartig, 2021), car (Fox and Weisberg, 2019), emmeans (Length, 2021), ggplot2 (Wickham, 2016). Generalised linear models with a binomial distribution and logit function were fitted to examine: (1) the effect of temperature on the probability of apothecia development on a rachis (section 2.2.1); (2) the effect of earlier rachis incubation temperature on the probability of apothecia development (section 2.2.2). The effect of temperature on the probability of apothecia development (1; section 2.2.1) was based on the presence of immature rather than mature apothecia, because mature apothecia were rarely formed in the dark. Only treatments with apothecia development were included in the analysis, because statistical description of results was not necessary for treatments where no apothecia developed. Significance of variables from models was assessed using type II likelihood ratio chi-square tests and $p < 0.05$ as a threshold for significance (NB likelihood ratio chi-square statistic = LR Chisq). *Post hoc* analyses of the models produced for (2) was conducted on the estimated marginal means of treatments, using Tukey's method for calculation of p values, with $p < 0.05$ as a threshold for significance. *Post hoc* analysis was not required for the model produced to analyse data from (1) because apothecia only developed in two treatments.

The effect of temperature on the timing of the maximum proportion of rachises bearing immature apothecia (section 2.2.1) was examined using the Wilcoxon rank sum test (NB Wilcoxon test statistic = W) with continuity correction. The effect of the earlier incubation temperature on the timing of the maximum proportion of rachises forming apothecia (section 2.2.2) was examined using a Kruskal-Wallis rank sum test, with a Wilcoxon rank sum test with continuity and Bonferroni correction for *post hoc* pairwise comparisons between treatments.

3. Results

3.1. Apothecia development in the field

3.1.1. Site characteristics and apothecia size and identification

Real-time PCR tests confirmed that apothecia and pseudosclerotial plates on collected rachises were produced by *H. fraxineus* (File S1). There was considerable variation in the production of apothecia both within and between sites throughout the sampling period (Fig. S2). The maximum apothecia area (total surface area of all cups) was mostly greater in 2019 (17 of the 24 sampling locations) compared with 2018 (7 of the 24 sampling locations). Higher values for apothecia area in 2019 corresponded with a greater median mean daily relative humidity at all sites in June and July 2019 than in 2018 (Fig. S3). In contrast, median mean daily temperatures were higher at all sites in June and July in 2018 than in 2019 (Fig. S4).

Within sites, there was some indication that in locations where rachises were under vegetation cover the maximum apothecia area tended to be higher, whereas in locations with only litter cover the maximum apothecia area was lower, but within site variability was high (Fig. S2). Gap fraction was related to ground cover type. Where vegetation cover tended to be most common, typically tree canopies were most open (i.e. gap fraction was greatest). Tree canopies were typically denser (i.e. gap fraction was lowest) in areas of moss cover, followed marginally by areas of bare soil and litter cover (Fig. S5).

3.1.2. Supported models

Removal of site as a random effect did not significantly affect models, therefore ΔAICc values of models including gap fraction and vegetation were calculated without site as a random effect for comparison of the value of fixed effects on model performance. Three models were identified with a ΔAICc value less than 7, and the final models were then constructed with site as a random effect where possible (Table 2; Fig. 2; Fig. 4; Fig. S6).

There was significant two-way interaction between mean temperature over the previous 14 d and mean relative humidity over the previous 7 d (apothecia model 1, $ddf = 368.19$, $p < 0.001$; apothecia model 2, $ddf = 371.49$, $p < 0.001$). As temperature increased, the effect of relative humidity became positive (Fig. 3; Fig. 5). In addition, the mean temperature over the previous 14 d significantly interacted with either the ground cover (apothecia model 1, $ddf = 370.54$, $p < 0.001$) or the gap fraction (apothecia model 2, $ddf = 377.10$, $p < 0.001$). Vegetation, soil and moss ground cover was correlated with greater apothecia development than with litter cover (Fig. 3), whilst a larger gap fraction (i.e. a more open canopy) was associated with greater apothecia development (Fig. 5). This was particularly apparent at warmer temperatures (e.g. 16.5 °C vs 14 °C) (Fig. 3; Fig. 5).

Contrary to other models, apothecia model 3 identified a significant three-way interactive effect between ground cover, the mean temperature 14 d prior to collection and the mean humidity 42 d prior to collection ($ddf = 360.36$, $p < 0.01$) (Table 2). However, this model contained patterns that were also difficult to explain. For example, the effect of increasing temperature on $\log_{10}(\sqrt{\text{total apothecia area}(\mu m^2)})$ became more positive as relative humidity increased with all ground cover types, except on moss, where the effect of increasing temperature became less positive (Fig. S7). However, the small sample size of moss study locations ($n = 3$) may have influenced this finding.

3.2. Apothecia development in the laboratory

3.2.1. Effect of incubation temperature

Numerous immature apothecia formed on rachises incubated at 15 °C and 20 °C, but not on rachises incubated at 4 °C or 10 °C. No

Table 2
Supported linear mixed effects models for *H. fraxineus* apothecia development ($\log_{10}(\sqrt{\text{apothecia area } (\mu m^2)})$) that had ΔAICc (Δ second-order Akaike Information Criterion) < 7 (Burnham et al., 2011).

Model	Fixed Effects[a]	p (ddf)	Random Effects	AICc[b]	ΔAICc[b]	Marginal R^2/Conditional R^2
Apothecia model 1	14 day mean temperature (°C): 7 day mean relative humidity (%) 14 day mean temperature (°C): Ground cover	<0.001 (368.19) <0.001 (370.54)	Site Quadrat Year	192.30	0	0.29/0.61
Apothecia model 2	14 day mean temperature (°C): 7 day mean relative humidity (%) 14 day mean temperature (°C): Gap fraction	<0.001 (371.49) <0.001 (377.10)	Quadrat Year	192.34	0.04	0.30/0.57
Apothecia model 3	14 day mean temperature (°C): Ground cover: 42 day mean relative humidity (%)	<0.01 (360.36)	Site Quadrat Year	195.57	3.27	0.30/0.65

[a] Fixed effects are listed at their highest interaction (: denotes an interaction) and p values were calculated using Kenward-Roger approximation for denominator degrees of freedom (ddf) (Luke, 2017).
[b] AICc and ΔAICc values were calculated not including site as a random effect to allow for comparison of fixed effects of models.

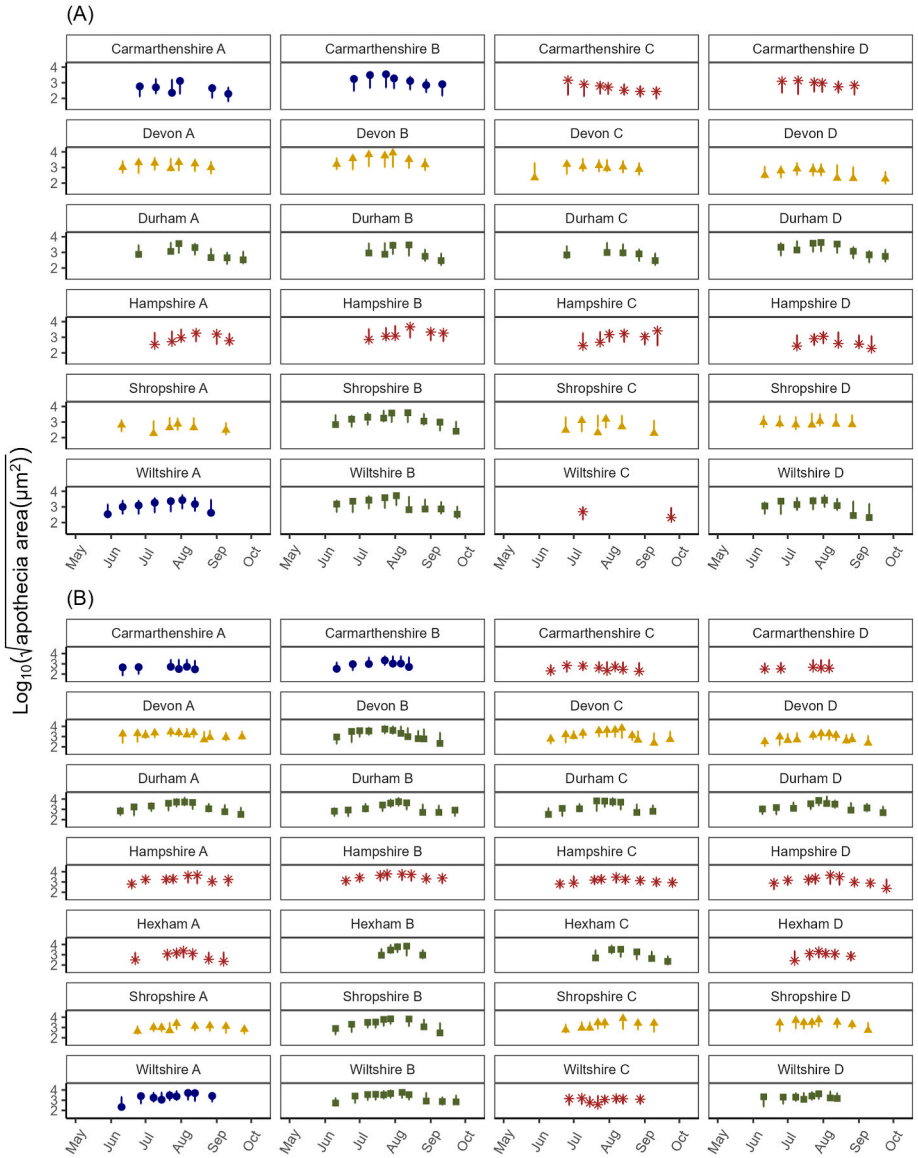

Fig. 2. Sum of the measured *H. fraxineus* apothecia area ($\log_{10}(\sqrt{\text{apothecia area } (\mu m^2)})$) with the 95 % confidence intervals of apothecia model 1 predictions. Ground cover is represented by ■ (vegetation), ● (moss), ▲ (bare soil) and ✳ (litter). **(A)** six sites in 2018 and **(B)** seven sites in 2019 with four plots at each site (A, B, C, D).

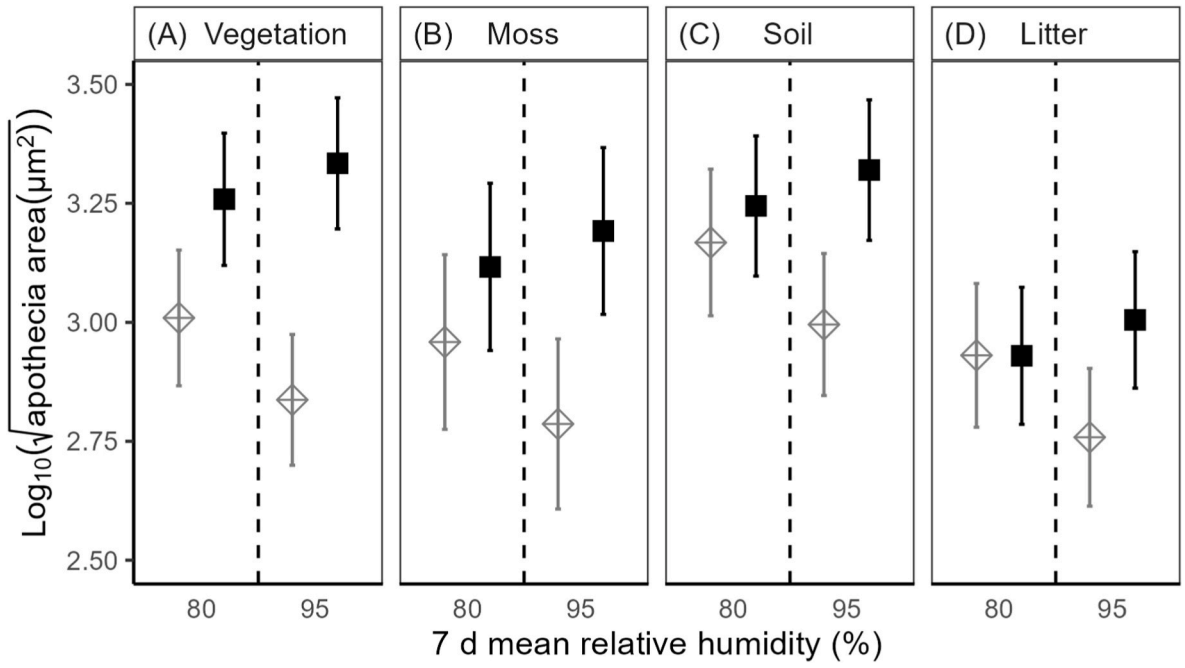

Fig. 3. Effect of temperature, relative humidity and ground cover ((**A)** vegetation, **(B)** moss, **(C)** bare soil, **(D)** litter) on the abundance of *H. fraxineus* apothecia at a sampling location ($\log_{10}(\sqrt{\text{apothecia area } (\mu m^2)})$) from apothecia model 1. Values are the estimated marginal means (and standard error) with temperature indicated by shape and shading of data (⟐ = 14 °C; ■ = 16.5 °C).

mature apothecia developed in the dark at 4 °C or 10 °C, but one rachis (out of 106) developed mature apothecia at 15 °C, and 16 (out of 102) developed mature apothecia at 20 °C.

The proportion of rachises that developed immature apothecia was not only significantly greater at 20 °C (median = 1.00, IQR = 0.07) than at 15 °C (median = 0.63, IQR = 0.27) (LR Chisq = 35.61, df = 1, $p < 0.001$) (Fig. S8), but also significantly quicker to reach the maximum (20 °C median = 53 d, IQR = 7 d; 15 °C median = 74 d, IQR = 7 d) (W = 47.5, $p < 0.01$) (Fig. 6).

3.2.2. *Effect of previous incubation temperature*

Holding at 4 °C, 10 °C, 15 °C or 20 °C in darkness then switching to 18–21 °C in the presence of daylight resulted in the abundant formation of mature apothecia on rachises. The temperature at which rachises were initially held also significantly affected the proportion that went on to develop mature apothecia (LR Chisq = 18.43, df = 3, $p < 0.001$), with rachises previously incubated at 4 °C significantly more likely to develop apothecia (median = 0.96, IQR = 0.08) than those previously incubated at either 15 °C (median = 0.75, IQR = 0.00) ($p < 0.001$) or 20 °C (median = 0.64, IQR = 0.13) ($p < 0.01$) (Fig. S9). In addition, the time taken for the maximum proportion of rachises to develop apothecia differed significantly between treatments (Kruskal-Wallis Chisq = 16.56, df = 3, $p < 0.001$). Rachises previously incubated at 4 °C took the most time (median = 66 d, IQR = 18 d) when compared with those initially held at 15 °C (median = 50 d, IQR = 6 d) or 20 °C (median = 44 d, IQR = 11 d) ($p < 0.05$) (Fig. 7).

3.2.3. *Interaction between light and threshold temperature*

Temperature in boxes of rachises incubated in darkness was the same temperature as incubator air temperature (10 °C). However, if boxes were not wrapped in foil, their internal temperature during the illumination period rose to 14.2 °C, resulting in a daily mean temperature of 13.1 °C. This meant that the effect of light could not be completely separated from temperature effect.

Nonetheless, immature apothecia were present after 9 wks on 75 of 105 rachises exposed to light (or 56 of 60 rachises if boxes were excluded that were poorly sealed and so allowed material to dry out). For boxes maintained at 10 °C in the dark (7 boxes), immature apothecia developed on only 3 out of 105 rachises after 9 wks, and on 11 out of 90 rachises (across 4 of 6 remaining boxes) after a further 10 wks incubation. Moreover, only a single rachis incubated in darkness at 10 °C developed more than 5 immature apothecia.

4. Discussion

Under field conditions, temperature, relative humidity, ground cover and gap fraction (a measure of tree canopy openness) all significantly influenced development of *H. fraxineus* apothecia. Furthermore, laboratory experiments under controlled conditions revealed that the rate of apothecia development increases with temperature. Additionally, maintaining rachises for about 3 months at 4, 10, 15 or 20 °C before exposing them to daylight and ambient temperatures showed that the subsequent rate of apothecia development is positively related to temperature, although more apothecia are likely to develop following a period of exposure to low temperature.

In our study we found that apothecia with a cup diameter of > 200 µm (i.e. those large enough to form a hymenium (Fig. S1)) were absent from woodlands when the mean temperature over the previous week was less than 12.2 °C; also that very limited apothecia development occurred at 10 °C in the laboratory, although as we only used fixed cardinal temperatures of 4 °C and 10 °C we were not able to pin-point the exact temperature at which apothecia development was completely inhibited. Our results indicate that low temperatures inhibit apothecia development and accord with observations that apothecia only form during late spring and summer months (Queloz et al., 2011; Mansfield et al., 2018), and that *H. fraxineus* spores are rarely detected on days when the mean daily temperature falls below 12 °C (Chandelier et al., 2014). Given a very small number of immature apothecia that developed on a maximum of only about 12 % of rachises incubated at 10 °C in our experiments, this suggests that most *H. fraxineus* individuals are unable to develop apothecia at this temperature, and that the threshold for *H. fraxineus* apothecia development is around 10 °C. A mean daily threshold temperature of ~10 °C for apothecia development would also synchronize pathogen fruiting and ascospore dispersal with

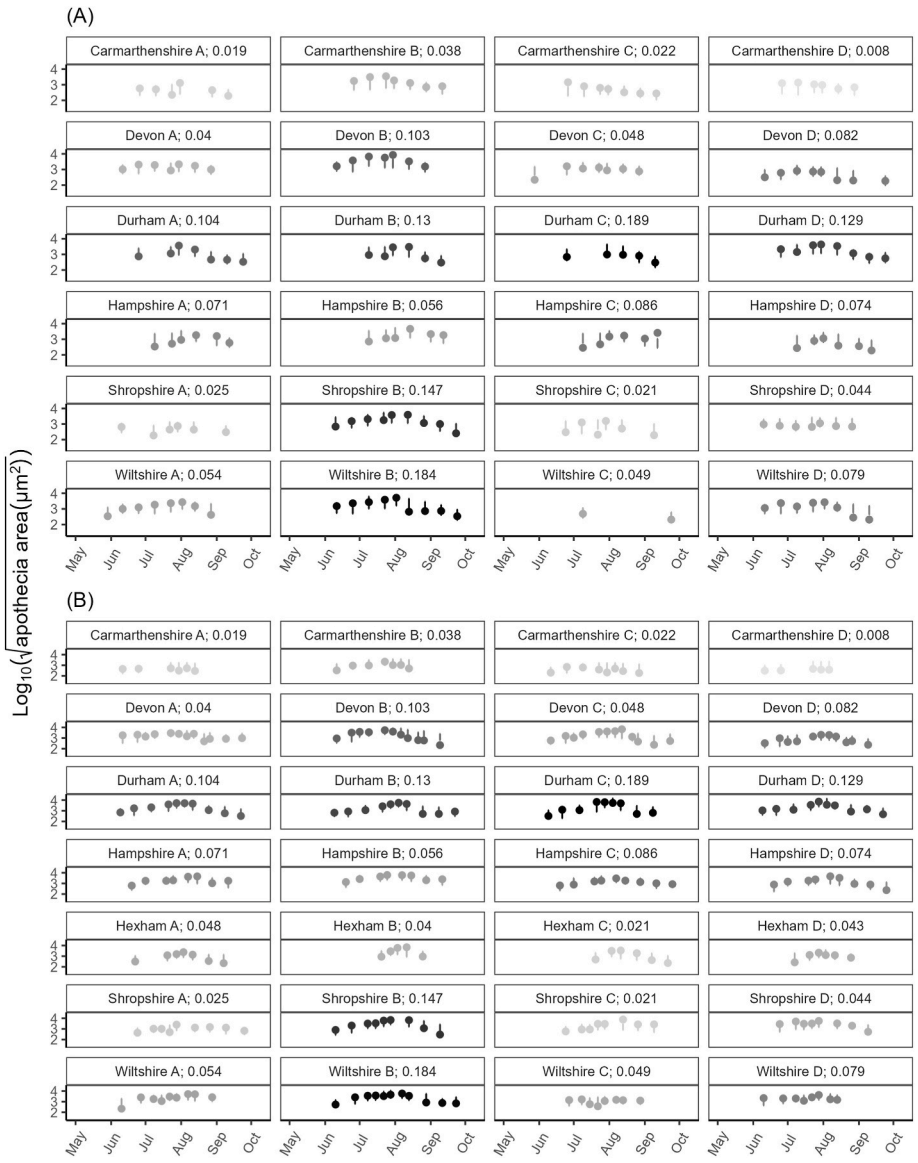

Fig. 4. Sum of the measured *H. fraxineus* apothecia area ($\log_{10}(\sqrt{\text{apothecia area } (\mu m^2)})$) with the 95 % confidence intervals of apothecia model 2 predictions. **(A)** six sites in 2018 and **(B)** seven sites in 2019 with four plots at each site (A, B, C, D), with gap fraction at a location presented in the panel titles and indicated by shading of datapoints (darkest points have the highest gap fraction).

availability of host tissue for infection (i.e. after leaf flushing).

Our findings also demonstrated that above the ~10 °C threshold, temperature positively affects the development of apothecia. Assuming that greater apothecia development will be associated with production of larger numbers of ascospores, our results are consistent with the positive correlation between higher annual temperatures (measured as degree days) and the maximum *H. fraxineus* ascospore quantity reported by Hietala et al. (2018). The maximum temperature for apothecia development and spore production has not been determined, but *in vitro* the optimum for mycelial extension is 20–22 °C (Hauptman et al., 2013) and only 10 % of *H. fraxineus* isolates grow at 30 °C (Kowalski and Bartnik, 2010). At our woodland sites, the maximum mean daily temperature recorded at 40 cm above ground level was 22.28 °C; this included unseasonably warm periods during both study years and indicates that even in UK 'heatwave' conditions, temperatures on the forest floor are unlikely to constrain apothecia development.

When models were developed to explore the interaction between environment and fruiting by *H. fraxineus*, the most supported models showed that the effect of a warmer temperature on apothecia development was dependent on relative humidity, ground cover and the gap fraction. Previous observations from Japan suggested that *H. fraxineus* apothecia were more abundant in areas that were shaded and humid rather than dry and sunny (Inoue et al., 2019). We found at warmer temperatures, ground cover associated with greater humidity also was most favourable to the formation of apothecia. For example, at 16.5 °C, apothecia development was greatest on rachises under vegetation, and somewhat enhanced on bare soil and moss when compared to rachises mixed with litter. When rachises are covered by vegetation they tend to be sheltered from direct solar radiation, reducing evaporation and retaining moisture at the ground surface. Although bare soil or moss do not offer the same environment, they are associated with a closed overhead tree canopy which will offer similar protection. Areas of open litter cover were also associated with closed overhead tree canopies, but litter itself is less able to retain moisture than either areas of moss or soil (albeit dependent on the soil type). This means that rachises in areas of open litter cover can be expected to be associated with lower humidity, resulting in greater desiccation of the rachises and reduced fruiting.

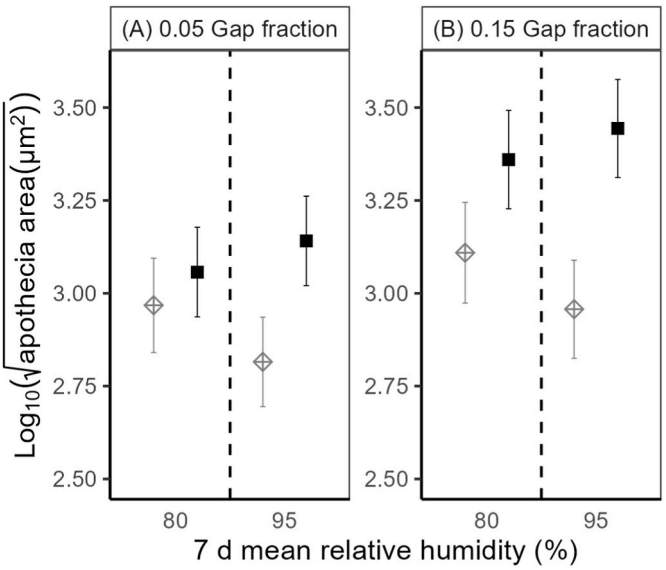

Fig. 5. Effect of mean temperature, mean relative humidity and gap fraction (**(A)** 0.05 gap fraction, **(B)** 0.15 gap fraction) on the abundance of *H. fraxineus* apothecia at a sampling location ($\log_{10}(\sqrt{\text{apothecia area } (\mu m^2)})$) from apothecia model 2. Values are the estimated marginal means (and standard error) with temperature indicated by shape and shading of data (⟐ = 14 °C; ■ = 16.5 °C).

The effect of ground cover on apothecia production has previously been associated with moisture availability. Fewer apothecia were recorded on open ground in UK woodlands compared to vegetation covered sites (Mansfield et al., 2018). Moreover, whilst no apothecia were found at an exposed site monitored over a single season in Switzerland, numerous apothecia formed when rachises were removed from the same site and incubated under humid conditions in the laboratory (Gross and Holdenrieder, 2013). Our results build on these previous findings, but by accounting for a wider range of variables also provide more quantitative estimates of the influence of different types of ground cover on apothecia development. In future, other studies could examine variations within the different types of litter and vegetation cover, with technologies such as remote sensing providing the tools (e.g. Yang et al., 2023) for application on a larger scale.

The finding that temperature has a more positive effect on apothecia development as the overhead canopy increases in openness appears counterintuitive but probably occurs because canopy openness is associated with increased ground-vegetation which in turn maintains humidity at the litter layer. Importantly, these results indicate a positive feedback in *H. fraxineus* infection. As the crowns of affected ash trees decline, greater gaps in the canopy appear, leading to increased *H. fraxineus* apothecia development and potentially greater inoculum density. Indeed, increasing relative light intensity in the understorey has previously been shown to be associated with more *H. fraxineus* infection on juvenile ash trees (Erfmeier et al., 2019).

Our results also demonstrate that relative humidity measured at 40 cm above ground level is significantly related to apothecia development. The large effect of moisture on apothecia development is supported through the impact of ground cover vegetation, canopy openness and greater apothecia development in 17 out of 24 study locations during a more humid study year. Moisture has previously been positively associated with apothecia abundance via flood risk index of sites (Grosdidier et al., 2018) and is consistently related to the increased development of ash dieback in woodlands (Marçais et al., 2016; Havrdová et al., 2017; Grosdidier et al., 2020; Klesse et al., 2021). Together, this emphasises the necessity of accurate measurement of moisture in the litter layer for developing models of apothecia development.

Conversely, at cooler temperatures (e.g. 14 °C), we found that the effect of relative humidity increasing from 80 % to 95 % had a negative impact on apothecia development. This could reflect different rates of apothecia senescence, although the factors that cause this have not been studied in *H. fraxineus*. Other organisms, including fungi, are associated with the decline of *H. fraxineus* apothecia (Kowalski and Bilański, 2022), and we observed nematodes feeding on rachises incubated in the laboratory for long periods.

Our laboratory findings also highlight how the long-term environment of a rachis between leaf fall in autumn and fruiting the following summer will influence the development of apothecia. Warmer 'pre-spring/summer' temperatures, simulated through a 17 wk incubation at 15 °C or 20 °C of *F. excelsior* rachises, reduces the time taken for apothecia development, concurring with a study in Norway which revealed a positive relationship between growing degree days and *H. fraxineus* ascospore quantities (Hietala et al., 2018). Additionally, a period of cool winter temperatures may be critical for optimal apothecia numbers as we found that rachises held at 4 °C were the most likely to go on to develop apothecia. It may also be that *H. fraxineus* has reduced metabolic activity at lower temperatures, so more resources are available for apothecia production later in the year. Taken together, these

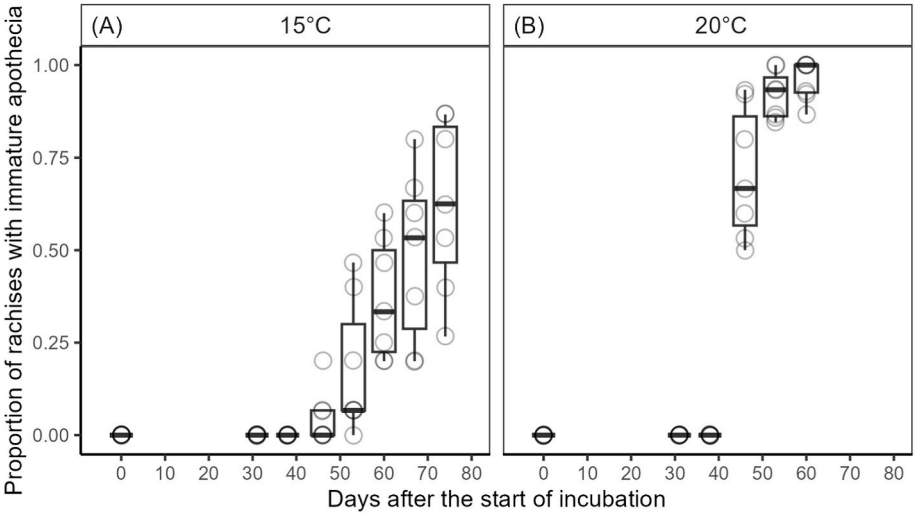

Fig. 6. Proportion of rachises producing immature apothecia under high humidity in darkness at **(A)** 15 °C (n = 7) and **(B)** 20 °C (n = 7). Datapoints are measured values from replicate boxes, and whiskers of boxplots represent values within 1.5*interquartile range of the upper or lower quantile.

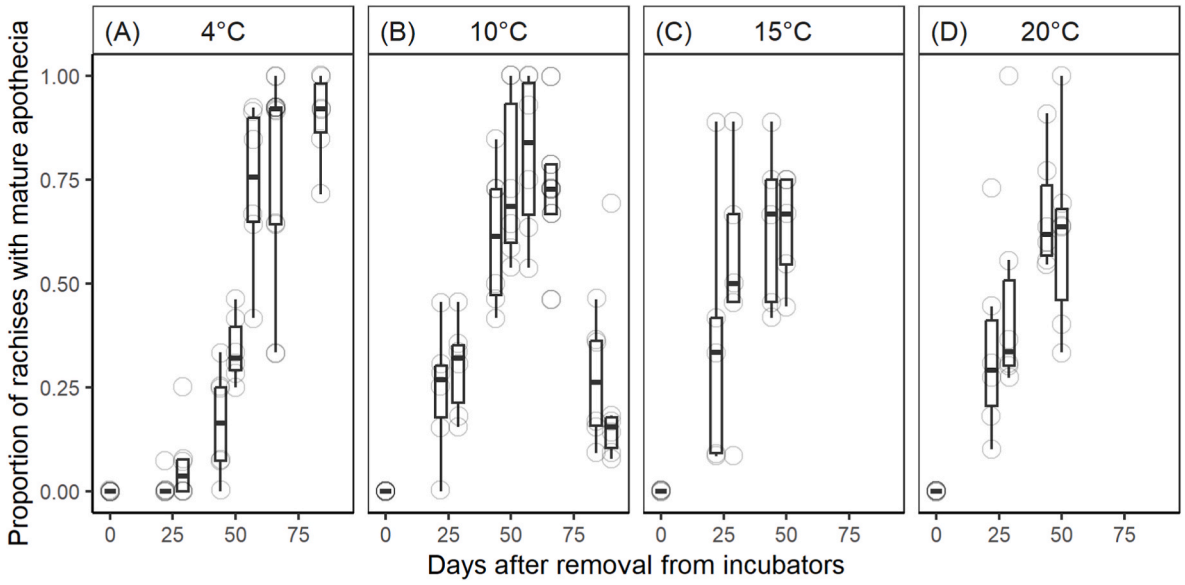

Fig. 7. Proportion of rachises producing mature apothecia of *H. fraxineus* following a switch to laboratory temperature (18–21 °C, with daylight and high humidity) from prior incubation at: **(A)** 4 °C (n = 6), **(B)** 10 °C (n = 6), **(C)** 15 °C (n = 5) and **(D)** 20 °C (n = 6) under high humidity in the dark for 17 wks. Datapoints are measured values from replicate boxes, and whiskers of boxplots represent values within 1.5*interquartile range of the upper or lower quantile.

findings indicate that a cumulative effect of environmental conditions acting on the fungus in rachises subsequently influences apothecia development and the lifecycle of *H. fraxineus*.

In conclusion, our results build on previous work by providing a more quantitative description of how *H. fraxineus* apothecia development is regulated by climatic (temperature, moisture) and site factors, such as canopy openness and ground cover. These interacting factors not only affect apothecia development but will ultimately affect inoculum production of *H. fraxineus*. Remaining variation in the models we developed can probably be explained by improving understanding of the effects of (1) microclimatic variation within woodlands, and (2) overwintering environment and rachis nutrient status on apothecia development. Although we identified ~10 °C as the threshold temperature for apothecia development, further laboratory incubation of *H. fraxineus* colonised rachises with different moisture and nutrient content across a range of temperatures, relative humidity, and light regimes would be needed to quantify their interactive effects on both development and senescence of apothecia. This information would contribute to more accurate development of process-based models of *H. fraxineus* lifecycle that could be used for disease prognosis and to quantify the impacts of disease control strategies.

CRediT authorship contribution statement

Matt Combes: Writing – review & editing, Writing – original draft, Visualization, Methodology, Investigation, Formal analysis, Conceptualization. **Lynne Boddy:** Writing – review & editing, Supervision, Methodology, Funding acquisition, Conceptualization. **Joan Webber:** Writing – review & editing, Supervision, Methodology, Funding acquisition, Conceptualization.

Disclosure

No use has been made of generative AI and AI-assisted technologies in the writing of this paper.

Funding

This work was supported by a grant for a PhD studentship to M.C. from Department for Environment, Food and Rural Affairs; Network Rail; and the Woodland Trust with additional funding from the Forestry Commission and Cardiff University.

Declaration of competing interest

The authors declare that they have no known competing financial interests or personal relationships that could have appeared to influence the work reported in this paper.

Acknowledgements

We thank all volunteers and woodland managers who were essential for the collection of the samples used in the study, and Jack Forster (Senior Statistician at Forest Research) for his advice on the statistical analyses.

Appendix A. Supplementary data

Supplementary data to this article can be found online at https://doi.org/10.1016/j.funeco.2025.101472.

References

Baral, H.-O., Bemmann, M., 2014. *Hymenoscyphus fraxineus* vs. *Hymenoscyphus albidus* - a comparative light microscopic study on the causal agent of European ash dieback and related foliicolous, stroma-forming species. Mycology 5, 228–290.

Baral, H.O., Queloz, V., Hosoya, T., 2014. *Hymenoscyphus fraxineus*, the correct scientific name for the fungus causing ash dieback in Europe. IMA Fungus 5, 79–80.

Barton, K., 2020. MuMIn: multi-model inference. R package version, 1.43.17. https://CRAN.R-project.org/package=MuMIn.

Bates, D., Maechler, M., Bolker, B., Walker, S., 2015. Fitting linear mixed-effects models using lme4. J. Stat. Software 67, 1–48.

Burnham, K.P., Anderson, D.R., Huyvaert, K.P., 2011. AIC model selection and multimodel inference in behavioral ecology: some background, observations, and comparisons. Behav. Ecol. Sociobiol. 65, 23–35.

Burns, P., Timmermann, V., Yearsley, J.M., 2022. Meteorological factors associated with the timing and abundance of *Hymenoscyphus fraxineus* spore release. Int. J. Biometeorol. 66, 493–506.

Buschbom, J., 2022. Genomic patterns and the evolutionary origin of an invasive fungal pathogen (*Hymenoscyphus fraxineus*) in Europe. Basic Appl. Ecol. 59, 4–16.

Caffi, T., Rossi, V., Legler, S.E., Bugiani, R., 2011. A mechanistic model simulating ascosporic infections by *Erysiphe necator*, the powdery mildew fungus of grapevine. Plant Pathol. 60, 522–531.

Čermáková, V., Kudláček, T., Rotková, G., Rozsypálek, J., Botella, L., 2017. *Hymenoscyphus fraxineus* mitovirus 1 naturally disperses through the airborne

inoculum of its host, *Hymenoscyphus fraxineus*, in the Czech Republic. Biocontrol Sci. Technol. 27, 992–1008.
Chandelier, A., Helson, M., Dvorak, M., Gischer, F., 2014. Detection and quantification of airborne inoculum of *Hymenoscyphus pseudoalbidus* using real-time PCR assays. Plant Pathol. 63, 1296–1305.
Cleary, M.R., Daniel, G., Stenlid, J., 2013. Light and scanning electron microscopy studies of the early infection stages of *Hymenoscyphus pseudoalbidus* on *Fraxinus excelsior*. Plant Pathol. 62, 1294–1301.
Combes, M., Webber, J., Boddy, L., 2024. Current understanding and future prospects for ash dieback disease with a focus on britain. Forestry 97, 678–691.
Dvorak, M., Rotkova, G., Botella, L., 2015. Detection of airborne inoculum of *Hymenoscyphus fraxineus* and *H. albidus* during seasonal fluctuations associated with absence of apothecia. Forests 7, 1.
Enderle, R., Nakou, A., Thomas, K., Metzler, B., 2014. Susceptibility of autochthonous German *Fraxinus excelsior* clones to *Hymenoscyphus pseudoalbidus* is genetically determined. Ann. For. Sci. 72, 183–193.
Erfmeier, A., Haldan, K.L., Beckmann, L.-M., Behrens, M., Rotert, J., Schrautzer, J., 2019. Ash dieback and its impact in near-natural forest remnants – a plant community-based inventory. Front. Plant Sci. 10, 658.
Fox, J., Weisberg, S., 2019. An R Companion to Applied Regression, third ed. Sage, Thousand Oaks, CA.
Fritsch, C., Grosdidier, M., Gégout-Petit, A., Marçais, B., 2024. Mechanistic-statistical model for the expansion of ash dieback. arXiv 2409, 06273.
George, J.P., Sanders, T.G.M., Timmermann, V., Potočić, N., Lang, M., 2022. European-wide forest monitoring substantiate the necessity for a joint conservation strategy to rescue European ash species (*Fraxinus* spp.). Sci. Rep. 12, 4764.
Gonsamo, A., D'odorico, P., Pellikka, P., 2013. Measuring fractional forest canopy element cover and openness – definitions and methodologies revisited. Oikos 122, 1283–1291.
Grosdidier, M., Ioos, R., Marçais, B., 2018. Do higher summer temperatures restrict the dissemination of *Hymenoscyphus fraxineus* in France? For. Pathol. 48, e12426.
Grosdidier, M., Scordia, T., Ioos, R., Marçais, B., 2020. Landscape epidemiology of ash dieback. J. Ecol. 108, 1789–1799.
Gross, A., Holdenrieder, O., 2013. On the longevity of *Hymenoscyphus pseudoalbidus* in petioles of *Fraxinus excelsior*. For. Pathol. 43, 168–170.
Hartig, F., 2021. DHARMa: residual diagnostics for hierarchical (Multi-Level/mixed) regression models. R package version 0.4.4. https://CRAN.R-project.org/package=DHARMa.
Hauptman, T., Piškur, B., Groot, M. de, Ogris, N., Ferlan, M., Jurc, D., 2013. Temperature effect on *Chalara fraxinea*: heat treatment of saplings as a possible disease control method. For. Pathol. 43, 360–370.
Havrdová, L., Zahradník, D., Romportl, D., Pešková, V., Černỳ, K., 2017. Environmental and silvicultural characteristics influencing the extent of ash dieback in forest stands. Balt. For. 23, 168–182.
Hietala, A.M., Børja, I., Solheim, H., Nagy, N.E., Timmermann, V., 2018. Propagule pressure build-up by the invasive *Hymenoscyphus fraxineus* following its introduction to an ash forest inhabited by the native *Hymenoscyphus albidus*. Front. Plant Sci. 9, 1087.
Hurvich, C.M., Tsai, C.-L., 1989. Regression and time series model selection in small samples. Biometrika 76, 297–307.
Husson, C., Caël, O., Grandjean, J.P., Nageleisen, L.M., Marçais, B., 2012. Occurrence of *Hymenoscyphus pseudoalbidus* on infected ash logs: occurrence of *Hymenoscyphus pseudoalbidus* on ash logs. Plant Pathol. 61, 889–895.
Inoue, T., Okane, I., Ishiga, Y., Degawa, Y., Hosoya, T., Yamaoka, Y., 2019. The life cycle of *Hymenoscyphus fraxineus* on Manchurian ash, *Fraxinus mandshurica*, in Japan. Mycoscience 60, 89–94.
Ioos, R., Fourrier, C., Iancu, G., Gordon, T., 2009b. Sensitive detection of *Fusarium circinatum* in pine seed by combining an enrichment procedure with a real-time polymerase chain reaction using dual-labeled probe chemistry. Phytopathology 99, 582–590.
Ioos, R., Kowalski, T., Husson, C., Holdenrieder, O., 2009a. Rapid in planta detection of *Chalara fraxinea* by a real-time PCR assay using a dual-labelled probe. Eur. J. Plant Pathol. 125, 329–335.
Kirisits, T., 2015. Ascocarp formation of *Hymenoscyphus fraxineus* on several-year-old pseudosclerotial leaf rachises of *Fraxinus excelsior*. For. Pathol. 45, 254–257.
Klesse, S., Abegg, M., Hopf, S.E., Gossner, M.M., Rigling, A., Queloz, V., 2021. Spread and severity of ash dieback in Switzerland – tree characteristics and landscape features explain varying mortality probability. Front. For. Glob. Change 4 (1–11), 645920.
Knowles, J.E., Frederick, C., 2020. merTools: tools for analyzing mixed effect regression models. R package version 0.5.2. https://CRAN.R-project.org/package=merTools.
Kowalski, T., 2006. *Chalara fraxinea* sp. nov. associated with dieback of ash (*Fraxinus excelsior*) in Poland. For. Pathol. 36, 264–270.
Kowalski, T., Bartnik, C., 2010. Morphologial variation in colonies of *Chalara fraxinea* isolated from ash (*Fraxinus excelsior* L.) stems with symptoms of dieback and effects of temperature on colony growth and structure. Acta Agrobot. 63, 99–106.
Kowalski, T., Bilański, P., 2021. Fungi detected in the previous year's leaf petioles of *Fraxinus excelsior* and their antagonistic potential against *Hymenoscyphus fraxineus*. Forests 12, 1412.
Kowalski, T., Bilański, P., 2022. Fungicolous fungi on pseudosclerotial plates and apothecia of *Hymenoscyphus fraxineus* and their biocontrol potential. Microorganisms 10, 2250.
Kuznetsova, A., Brockhoff, P.B., Christensen, R.H.B., 2017. lmerTest package: tests in linear mixed effects models. J. Stat. Software 82, 1–26.
Laubray, S., Buée, M., Marçais, B., 2023. Evidence of a component allee effect for an invasive pathogen: *Hymenoscyphus fraxineus*, the ash dieback agent. Biol. Invasions 25, 2567–2582.
Length, R.V., 2021. Emmeans: estimated marginal means, Aka least-squares means. R package version 1.7.0. https://CRAN.R-project.org/package=emmeans.
Luke, S.G., 2017. Evaluating significance in linear mixed-effects models in R. Behav. Res. Methods 49, 1494–1502.
Mansfield, J.W., Galambos, N., Saville, R., 2018. The use of ascospores of the dieback fungus *Hymenoscyphus fraxineus* for infection assays reveals a significant period of biotrophic interaction in penetrated ash cells. Plant Pathol. 67, 1354–1361.
Marçais, B., Husson, C., Godart, L., Caël, O., 2016. Influence of site and stand factors on *Hymenoscyphus fraxineus* induced basal lesions. Plant Pathol. 65, 1452–1461.
McKinney, L.V., Nielsen, L.R., Hansen, J.K., Kjær, E.D., 2011. Presence of natural genetic resistance in *Fraxinus excelsior* (Oleraceae) to *Chalara fraxinea* (Ascomycota): an emerging infectious disease. Heredity 106, 788–797.
Nakagawa, S., Schielzeth, H., 2013. A general and simple method for obtaining R^2 from generalized linear mixed-effects models. Methods Ecol. Evol. 4, 133–142.
Nemesio-Gorriz, M., McGuinness, B., Grant, J., Dowd, L., Douglas, G.C., 2019. Lenticel infection in *Fraxinus excelsior* shoots in the context of ash dieback. iForest 12, 160.
Queloz, V., Grünig, C.R., Berndt, R., Kowalski, T., Sieber, T.N., Holdenrieder, O., 2011. Cryptic speciation in *Hymenoscyphus albidus*. For. Pathol. 41, 133–142.
R Core Team, 2021. R: a Language and Environment for Statistical Computing. R Foundation for Statistical Computing, Vienna, Austria. URL. https://www.R-project.org/.
Rossi, V., Giosuè, S., Bugiani, R., 2007. A-scab (Apple-scab), a simulation model for estimating risk of *Venturia inaequalis* primary infections. EPPO Bull. 37, 300–308.
Schneider, C.A., Rasband, W.S., Eliceiri, K.W., 2012. NIH image to ImageJ: 25 years of image analysis. Nat. Methods 9, 671–675.
Spiess, A.-N., 2018. qpcR: modelling and analysis of real-time PCR data. R package version 1, 4-1. https://CRAN.R-project.org/package=qpcR.
Stocks, J.J., Buggs, R.J.A., Lee, S.J., 2017. A first assessment of *Fraxinus excelsior* (common ash) susceptibility to *Hymenoscyphus fraxineus* (ash dieback) throughout the British Isles. Sci. Rep. 7, 16546.
Wickham, H., 2016. ggplot2: Elegant Graphics for Data Analysis. Springer-Verlag, New York.
Wouters, H., 2021. Downscaled bioclimatic indicators for selected regions from 1979 to 2018 derived from reanalysis. Copernicus Climate Change Service (C3S) Climate Data Store (CDS). https://doi.org/10.24381/cds.fe90a594. (Accessed 21 April 2025).
Yang, X., Qiu, S., Zhu, Z., Rittenhouse, C., Riordan, D., Cullerton, M., 2023. Mapping understory plant communities in deciduous forests from Sentinel-2 time series. Remote sens. Environ. 293 (1–21), 113601.